



**HAL**  
open science

## First on-sky tests of LQG control for a 10m-class telescope: prelude on the Gran Telescopio Canarias adaptive optics system

Lucas Marquis, Henri-François Raynaud, Nicolas Galland, Jose Marco de la Rosa, Icíar Montilla Garcia, Óscar Tubío, Marcos Reyes García-Talavera, Gianluca Lombardi, Manuel Huertas Lopez, Daniel Reverte, et al.

### ► To cite this version:

Lucas Marquis, Henri-François Raynaud, Nicolas Galland, Jose Marco de la Rosa, Icíar Montilla Garcia, et al.. First on-sky tests of LQG control for a 10m-class telescope: prelude on the Gran Telescopio Canarias adaptive optics system. Adaptive Optics Systems IX, Jun 2024, Yokohama, Japan. pp.130977Y, 10.1117/12.3020099 . hal-04734161

**HAL Id: hal-04734161**

**<https://iogs.hal.science/hal-04734161v1>**

Submitted on 15 Oct 2024

**HAL** is a multi-disciplinary open access archive for the deposit and dissemination of scientific research documents, whether they are published or not. The documents may come from teaching and research institutions in France or abroad, or from public or private research centers.

L'archive ouverte pluridisciplinaire **HAL**, est destinée au dépôt et à la diffusion de documents scientifiques de niveau recherche, publiés ou non, émanant des établissements d'enseignement et de recherche français ou étrangers, des laboratoires publics ou privés.

# First on-sky tests of LQG control for a 10m-class telescope: prelude on the Gran Telescopio Canarias Adaptive Optics system

Lucas Marquis<sup>a</sup>, Henri-François Raynaud<sup>a</sup>, Nicolas Galland<sup>a</sup>, José Marco de la Rosa<sup>b</sup>, Icíar Montilla<sup>b</sup>, Óscar Tubío Araújo<sup>b</sup>, Marcos Reyes García-Talavera<sup>b</sup>, Gianluca Lombardi<sup>c</sup>, Manuel Huertas Lopez<sup>c</sup>, Daniel Reverte<sup>c</sup>, and Caroline Kulcsár<sup>a</sup>

<sup>a</sup>Institut d'Optique Graduate School, Laboratoire Charles Fabry - CNRS, Université Paris-Saclay, Palaiseau, France

<sup>b</sup>Instituto de Astrofísica de Canarias, La Laguna, Spain

<sup>c</sup>Gran Telescopio Canarias S.A., Spain

## ABSTRACT

The Gran Telescopio Canarias (GTC) is being equipped with an Adaptive Optics (AO) system,<sup>1</sup> developed by the Instituto de Astrofísica de Canarias (IAC).<sup>2</sup> The Institut d'Optique Graduate School-Laboratoire Charles Fabry (IOGS-LCF), through a collaboration with the IAC, integrated some high performance control solutions.<sup>3</sup> In this proceeding, we present the first and promising on-sky results on a 10-meter class telescope for such a controller, namely a full Linear Quadratic Gaussian regulator (LQG). We start with a brief description of the GTCAO system, including the data-driven LQG regulator construction. Performance results are then presented with a full LQG regulator in line with the previous on-bench experiments,<sup>3</sup> implemented in DARC,<sup>4</sup> the GTCAO RTC. A comparison is performed with the integrator, the baseline controller, through the comparison of point spread functions acquired on the scientific camera and residual slopes recorded by the wavefront sensor.

**Keywords:** Adaptive Optics, discrete-time LQG control, asymptotic Kalman filter, vibration filtering

## 1. INTRODUCTION

### 1.1 GTC telescope and GTCAO system

The Gran Telescopio Canarias is until now the biggest telescope in visible/infrared wavelength range. Located in La Palma (Canary Islands, Spain), it has a segmented primary mirror (36 segments) of equivalent diameter 10.4m. It is being equipped with an adaptive optics system: the GTCAO, a Single Conjugated AO (SCAO) system that was developed at the Instituto de Astrofísica de Canarias (IAC). It is composed of three main components. The wavefront sensor (WFS) is a Shack-Hartmann with a grid of micro-lenses of size  $20 \times 20$  and an OCAM2 camera (EMCCD). The measurement vector  $y$  has 624 components (312 used subapertures, shown in figure 1, left). The deformable mirror (DM) is a Cilas piezo-electric one of size  $21 \times 21$  with 373 used actuators (including the M2-obstructed ones, as shown in figure 1, right). Eventually, the real-time controller, namely the Durham AO Real-Time Controller<sup>4</sup> (DARC), embeds an LQG module. The system was defined and calibrated for loop sampling frequencies extending from 50 Hz to 1000 Hz. The correction of tip and tilt modes is assisted by the GTC secondary mirror, with an independent integrator control system that is not discussed in this article.

---

Further author information: lucas.marquis@institutoptique.fr

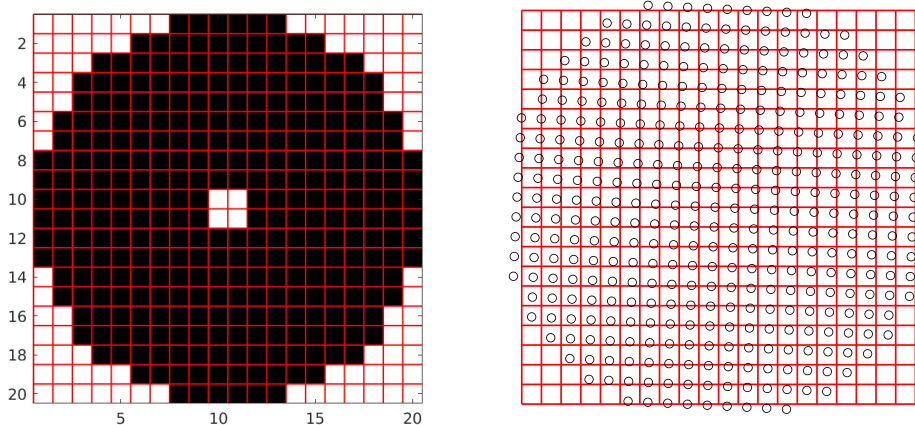


Figure 1: Left: 2D representation of the microlenses grid (red) with the 312 used subapertures of the GTCOA Shack-Hartmann WFS (black). Right: 2D representation of the GTCOA DM actuators positions (black circles) relatively to the microlenses grid (red, extracted from<sup>3</sup>).

## 1.2 GTCOA controller: towards auto-tuned data-driven LQG control

The baseline controller for GTCOA is an integrator. A high-performance data-driven controller has also been designed, specifically an LQG controller and associated state-space model.

### 1.2.1 Leaky integrator

When closing the loop with a sampling time of  $T_s$ , the integrator command  $u^{\text{INT}}$  at time  $kT_s$  is calculated using the residual wavefront slopes measurement  $y_k$  as follows:

$$u_k^{\text{INT}} = \alpha_{\text{leaky}} u_{k-1}^{\text{INT}} - g M_{\text{com}} y_k, \quad (1)$$

where  $M_{\text{com}}$  is the DM command matrix and  $\alpha_{\text{leaky}}$  the leakage factor of value 0.99. During the two observation nights we are describing the results of, the loop gain was set to  $g = 0.3$  for bright stars (April 25th 2024) and  $g = 0.5$  for faint stars (April 26th 2024).

### 1.2.2 Linear Quadratic Gaussian controller

The LQG is a high-performance controller designed to minimize the residual phase variance. As detailed in the SPIE 2022 proceeding,<sup>5</sup> it combines a state-space representation of the system dynamics with a Kalman filter to provide real-time prediction and correction of wavefront distortions. The state space representation matrices are built by following the procedure in L. Marquis PhD.<sup>3</sup> This thesis includes on-lab validation tests to assess performance and stability of the LQG regulator in presence of vibrations and measurement noise. We briefly precise in this section what are the main system and disturbance models that are intervening.

**System modelling** The GTCOA system was beforehand calibrated and modelled with on-lab data (internal source),<sup>3</sup> with notably a deformable mirror influence functions matrix  $N$  derived from a pseudo-synthetic interaction matrix, and an estimation of the fractional delay (used notably to define a state-to-command projector and to compute pseudo-open-loop slopes). Some extensive work has been done recently for the fractional loop delay modelling,<sup>6</sup> but it has not been implemented yet during the preliminary tests described in this paper. The WFS measurement noise covariance matrix is computed online during the night from WFS data.<sup>5</sup> If updated often enough, it accounts for M1 segmentation and rotation: the pupil is not circular and it is rotating throughout the night (due to the de-rotator) with a speed that depends on the elevation, and thus on the target. We can see this rotation in figure 2.

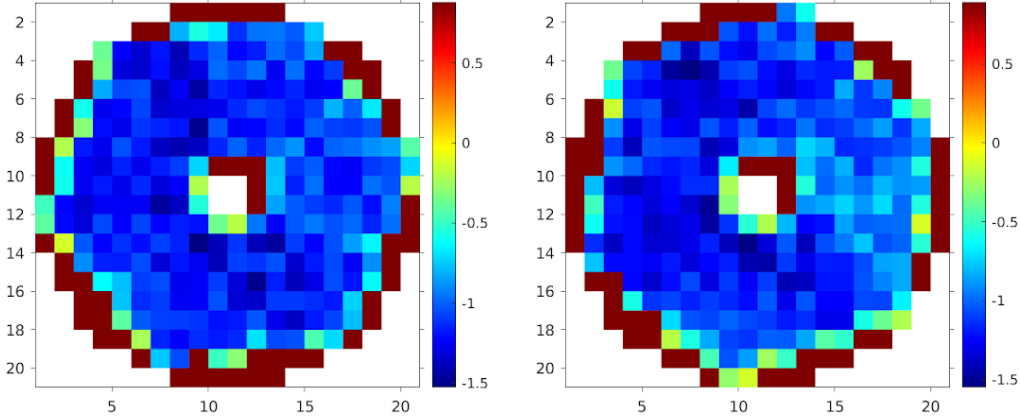


Figure 2: Two measurement noise covariance matrices in 2D pupil plan, using data samples recorded with a 10-minute gap. One can see a 15-degree spin (de-rotator). Log scale: outside subapertures are discarded by attributing to the corresponding noise variance 100 times bigger values than the median of illuminated ones.

**Disturbance modelling** The distorted wavefront is described in the Zernike basis with 665 modes.

- For the low orders from 1 to 9, the temporal state-space model of total order 144 is built using N4SID algorithm<sup>7</sup> ("model free") with enforced stability, successfully used on sky in 2019.<sup>8</sup> An example of corresponding power spectral density (PSD) is given in figure 3.

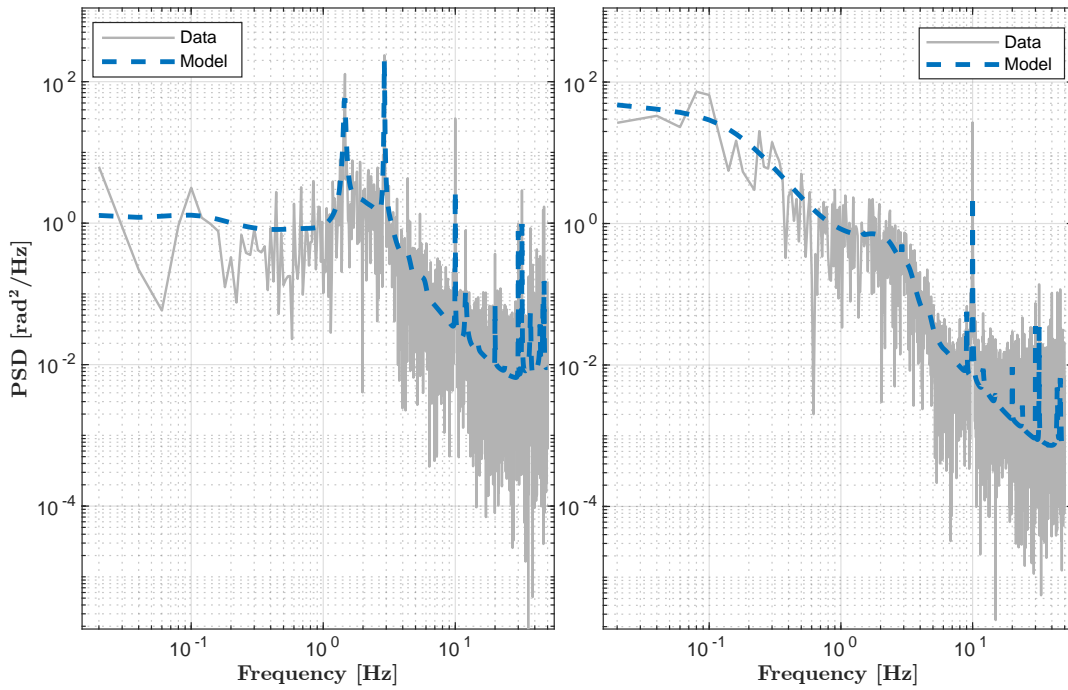


Figure 3: Examples of N4SID model (modes 1 and 5)

- For higher-order Zernike modes, an AR2 model is built,<sup>9</sup> based on atmosphere priors: Fried parameter, large scale factor and wind speeds, themselves deduced from telemetry data.<sup>3</sup>

## 2. FIRST ON-SKY RESULTS WITH LQG REGULATOR

We present here the first results obtained on sky when closing the loop with an LQG controller, in comparison with an integrator.

### 2.1 Correction performance

We see in figure 4 that the LQG regulator allowed to diminish the residual phase in the night of April 25th, with even stronger advantages for more challenging atmosphere (smaller  $r_0$ ). During that night, the NGSs' magnitudes were below 8, allowing for high sampling frequency (500 Hz or 1000 Hz).

For the night of April 26th, with results in figures 5 and 6, the NGSs' magnitudes were above 12 and the sampling frequencies were set to 200 Hz or 100 Hz. As a result, the integrator could not effectively tackle the vibrations while the LQG succeeded in strongly mitigating them, leading to a strong reduction of about 60 nm rms in the residual wavefront error. Profiles corresponding to PSFs in figure 6 are displayed in figure 7. They show that the LQG controller allowed to more than double the peak of intensity and sharpened the FWHM from 120 mas to 45 mas (co-phasing error excluded) during this second night (sampling frequency of 100 Hz). The FWHM of the diffraction-limited PSF is of 33 mas.

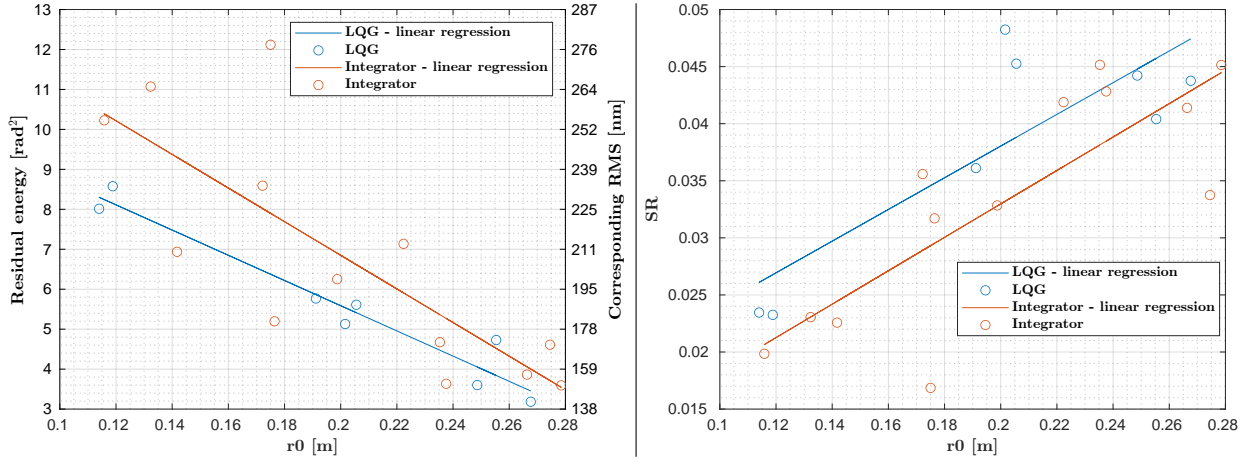


Figure 4: On-sky results of the night of April 25th 2024. Left: residual phase variance. Right: Strehl ratios at 1.6  $\mu\text{m}$ . Performance is globally critically diminished by M1 co-phasing errors.

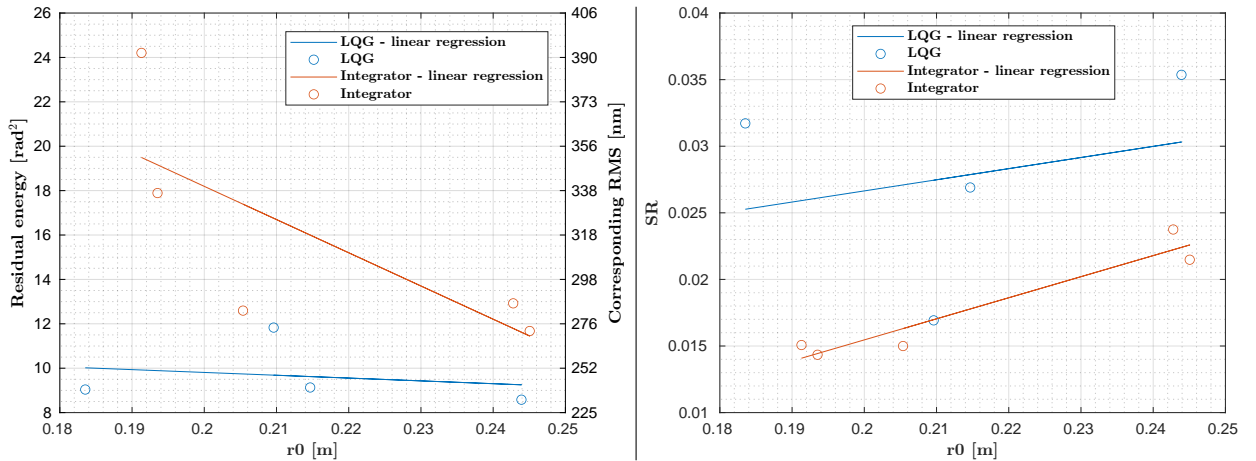


Figure 5: On-sky results of the night of April 26th 2024. Left: residual phase variance. Right: Strehl ratios at 1.6  $\mu\text{m}$ . Performance is globally critically diminished by M1 co-phasing errors.

It can be seen in figure 6 that the M1 segmented mirror was not well co-phased yet. As a result, the SRs are globally much lower than expected. Also, for both nights, the LQG tests were performed with sometimes strong delays between the matrices calculation and the on-sky closed-loop operation, likely leading to an underestimation of the performance.



Figure 6: Scientific images (11 mas/px, 1.6  $\mu\text{m}$ , 2-minute long exposure, magnitude 12.8) in closed-loop with the LQG (left, 1:30am,  $r_0$  at 500 nm = 17 cm) and the integrator (right, 1:15am,  $r_0$  at 500 nm = 18 cm).

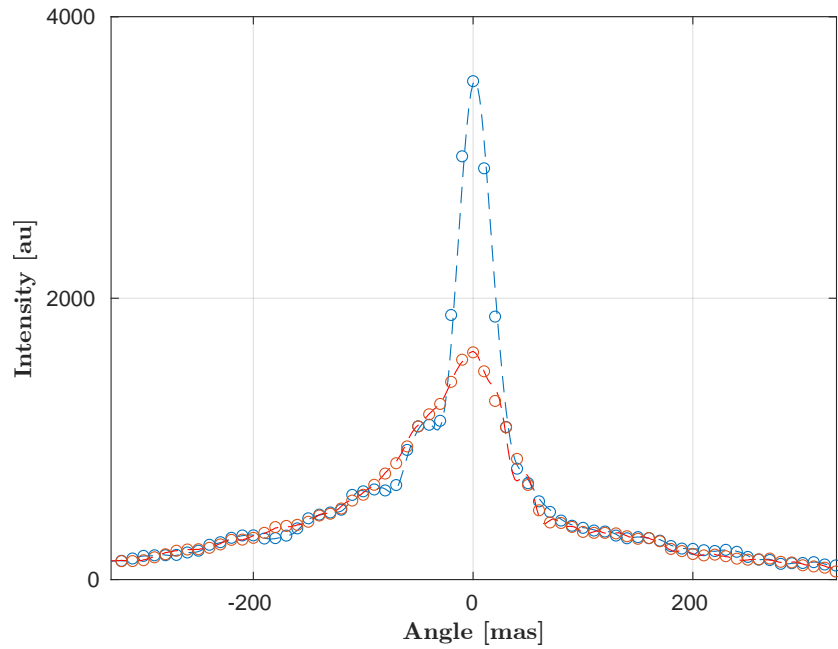


Figure 7: Profiles of the PSFs corresponding to figure 6 obtained with integrator (red) and LQG regulator (blue).

## 2.2 Spectral analysis

We consider here the case with an NGS of magnitude 12, with 100 FPS sampling rate. In the PSDs of figure 8, we notice that the LQG (blue) rejects the vibrations identified in figure 3. Those degrade the integrator (red) performance, not only for tip and tilt modes: the astigmatism is shown here, on the right, but some other low-order Zernike modes are also impacted.

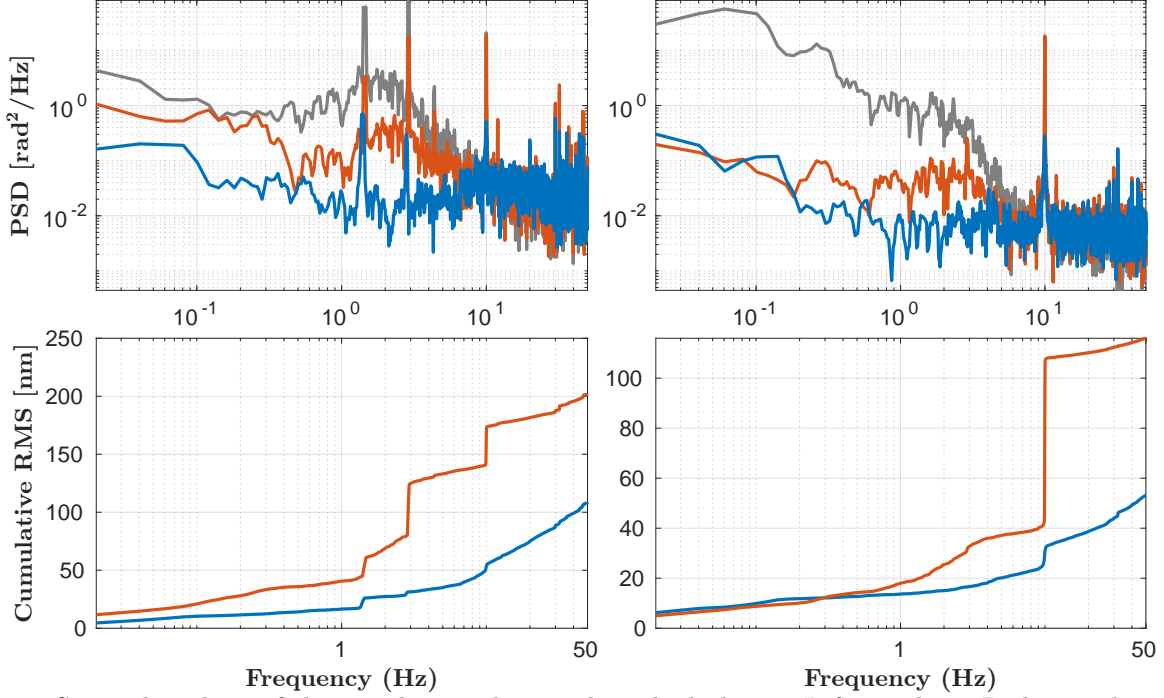


Figure 8: Spectral analysis of the pseudo-open-loop and residual phases. Left: mode 1. Right: mode 5. Top: PSD. Bottom: cumulative PSD. Blue: LQG. Red: integrator. Gray: pseudo-open-loop.

## 2.3 GTCAO DM actuators' stress

When operating with a well-tuned LQG regulator, the actuators' stroke STD did not go above  $0.2 \mu\text{m}$ , as shown in figure 9. This corresponds to less than 15% of the clipping value ( $1.4 \mu\text{m}$ ). With a global STD more than 5 times smaller than the integrator, the DM shape is much smoother. The integrator has thus more clipped commands values.

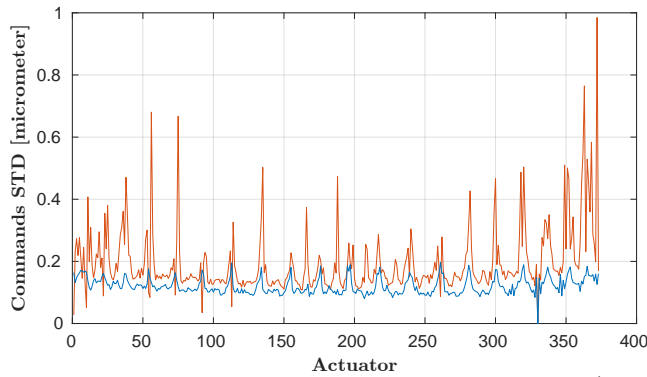


Figure 9: Example of actuators stroke temporal rms for the LQG regulator (blue) and the integrator (red).

### 3. CONCLUSION

In this proceeding, we have presented the first on-sky results with full LQG AO control on a 10-m class telescope, the Gran Telescopio Canarias, equipped with the GTCAO system. These preliminary results validate our LQG controller design, calibration and identification strategies, and implementation. As predicted by the IAC laboratory tests and replay simulations, the on-sky performance shows a significant improvement in both the Strehl ratio and the Full Width at Half Maximum compared to the integrator. A large portion of the integrator error budget is due to vibration. The error budget evaluation for both the integrator and the LQG<sup>10</sup> will need to be evaluated. These initial tests have also shown that the LQG performance comes with hardware advantages, with impressively reduced command strokes. These preliminary results will be complemented this year by more complete on-sky campaigns with optimal LQG and appropriate model updates.

### ACKNOWLEDGMENTS

This work is supported by the “Investissements d’Avenir” project funded by the IDEX Paris-Saclay, ANR-11-IDEX-0003-02. This project has received funding from the European Union’s Horizon 2020 research and innovation program, ORP Pilot, under grant agreement No 101004719.

### REFERENCES

- [1] Reyes García-Talavera, M., Montilla, I., Puga, M., López, R., González, E., Luis Simoes, R., Tubío, O., Marco, J., Josefina, R., Luis Aznar, M., Patrón, J., Sánchez-Béjar, V., Lombardi, G., de Paz, H., Reverte, D., Rodríguez, L., Cabrera, A., Huertas López, M., Fernández, S., Martín, M., González, P., Leal, A., and Navarro, S., “GTC adaptive optics integration in telescope and commissioning results,” *SPIE* (2024).
- [2] Montilla, I., de la Rosa, J. M., Tubío Araújo, Ó., Rosich, J., Reyes García-Talavera, M., Aznar, M. L., González, E., López, R., Simoes, R., Patrón Recio, J., Puga, M., and Sánchez Béjar, V., “Laboratory acceptance and telescope integration readiness of the Gran Telescopio Canarias adaptive optics system,” <https://doi.org/10.1117/12.2630109> **12185**, 660–667, *SPIE* (2022).
- [3] Marquis, L., *High-performance adaptive optics control for the Gran Telescopio Canarias*, PhD thesis, Université Paris Saclay and Universidad de La Laguna (2023). Instrumentation and Methods for Astrophysics [astro-ph.IM]. English. NNT : 2023UPAST087. tel-04278448.
- [4] Basden, A., Geng, D., Myers, R., and Younger, E., “Durham adaptive optics real-time controller,” *Applied Optics* **49**, 6354–6363 (2010).
- [5] Marquis, L., Kulcsár, C., Montilla, I., Raynaud, H.-F., Marco, J., Tubío, Ó., Basden, A., and Reyes, M., “Linear Quadratic Gaussian predictive control for the Gran Telescopio Canarias AO system: design issues and first bench results,” <https://doi.org/10.1117/12.2630257> **12185**, 909–916, *SPIE* (2022).
- [6] Marquis, L., Raynaud, H.-F., Galland, N., de la Rosa, J. M., Montilla, I., Óscar Tubío Araújo, García-Talavera, M. R., and Kulcsár, C., “Fractional loop delays in adaptive optics modeling and control,” *J. Opt. Soc. Am. A* **41**(1), 111–126 (2024).
- [7] Van Overschee, P. and De Moor, B., “N4sid: Subspace algorithms for the identification of combined deterministic-stochastic systems,” *Automatica* **30**(1), 75–93 (1994). Special issue on statistical signal processing and control.
- [8] Siquin, B., Prengere, L., Kulcsár, C., Raynaud, H.-F., Gendron, E., Osborn, J., Basden, A., Conan, J.-M., Bharmal, N., Bardou, L., et al., “On-sky results for adaptive optics control with data-driven models on low-order modes,” *Monthly Notices of the Royal Astronomical Society* **498**(3), 3228–3240 (2020).
- [9] Sivo, G., Kulcsár, C., Conan, J.-M., Raynaud, H.-F., Gendron, É., Basden, A., Vidal, F., Morris, T., Meimon, S., Petit, C., Gratadour, D., Martin, O., Hubert, Z., Sevin, A., Perret, D., Chemla, F., Rousset, G., Dipper, N., Talbot, G., Younger, E., Myers, R., Henry, D., Todd, S., Atkinson, D., Dickson, C., and Longmore, A., “First on-sky SCAO validation of full LQG control with vibration mitigation on the CANARY pathfinder,” *Optics Express* **22**(19), 23565 (2014).
- [10] Juvénal, R., Kulcsár, C., Raynaud, H.-F., and Conan, J.-M., “Linear controller error budget assessment for classical adaptive optics systems,” *Journal of the Optical Society of America. A Optics, Image Science, and Vision* **35**(8), 1465–1476 (2018).